Prediction and Correlation of Accessible Area of Large Multiparticle Aggregates

Daniel E. Rosner and Pushkar Tandon
Dept. of Chemical Engineering, High Temperature Chemical Reaction Engineering Laboratory,
Yale University, New Haven, CT 06520

Aggregates (composed of large numbers of primary particles) are produced in many engineering environments. One convenient characterization is the fractal dimension, the exponent describing how the number of primary particles in each aggregate scales with radial distance from its center of mass. We describe a finite-analytic pseudo-continuum prediction of the normalized accessible surface area of an isothermal quasi-spherical fractal aggregate containing N ($\gg 1$) primary particles, on the surfaces of which a first-order chemical process occurs. Results are displayed for specific fractal dimensions (2.5, 2.18, and 1.8) frequently observed in aggregating systems. An effective Thiele modulus is used to develop an efficient and accurate scheme for predicting/correlating the effectiveness factor for an aggregate containing N primary particles in terms of aggregate fractal dimension, reaction probability, and Knudsen number. Our methods now allow calculations of the accessible surface area of populations of aggregates, provided pdf{N, D_f, ...} is known for the populations of interest.

Introduction

In many technologies involving suspensions the dispersed phase is comprised of aggregated or agglomerated particles, themselves comprised of a large number, N, of primary particles or spherules which have coagulated (usually as the result of their Brownian motion). While the resulting aggregates may be quasi-spherical and compact, with relatively sharp, if irregular boundaries, more often they are sparse, apparently random clusters of spherules quite permeable to the surrounding solvent and its molecular solutes (Figure 1). Probably the most studied example is that of carbonaceous soot formed deliberately or inadvertently in the combustion of hydrocarbon fuels using air as a gaseous oxidizer (Medalia and Hickman, 1960; Siegla and Smith, 1981). However, qualitatively similar aggregated smokes arise in the vapor phase synthesis of inorganic pigments [for example, TiO_2(s)] or viscosity modifiers (for example, fumed silica) (Ulrich, 1984; Megaridis and Dobbins, 1990), and in the combustion of metals (for example, in flares or chemical flash lamps), or the production of catalytic materials (Formenti et al., 1972).

Predictions of the performance of systems containing such aggregates require a quantitative understanding of the laws governing the exchange of mass-, energy-, and/or momentum between each aggregate and the prevailing host fluid. In particular, we address here the question of what fraction of the surface area of the primary spherules is in fact *accessible* to a diffusing solute molecule in the "continuous" solvent phase—a high temperature combustion gas mixture in the above mentioned examples. For example, in the case of carbonaceous soot aggregates this fundamental question arises in, say, calculating the *growth* rate of the primary particles due to C_2H_2(g) molecule impacts, the *adsorption rate* of possibly carcinogenic condensible molecules, or the ultimate *oxidation rate* of the aggregates due to such combustion gas species as OH(g), O(g), O_2(g), CO_2(g), and so on. For more volatile materials the present theory could also be used to estimate large aggregate *sublimation* rates.

For *small* aggregates, comprised of only a few primary particles (say $2 < N < 20$) in a specified geometrical configuration (for example, linear chain, or quasi-spherical packing of uniform density, and so on) it is no longer impractical to make detailed calculations of transport phenomena in the complex shaped space exterior to the primary particles (Rosner et al.,

Correspondence concerning this article should be addressed to D. E. Rosner.

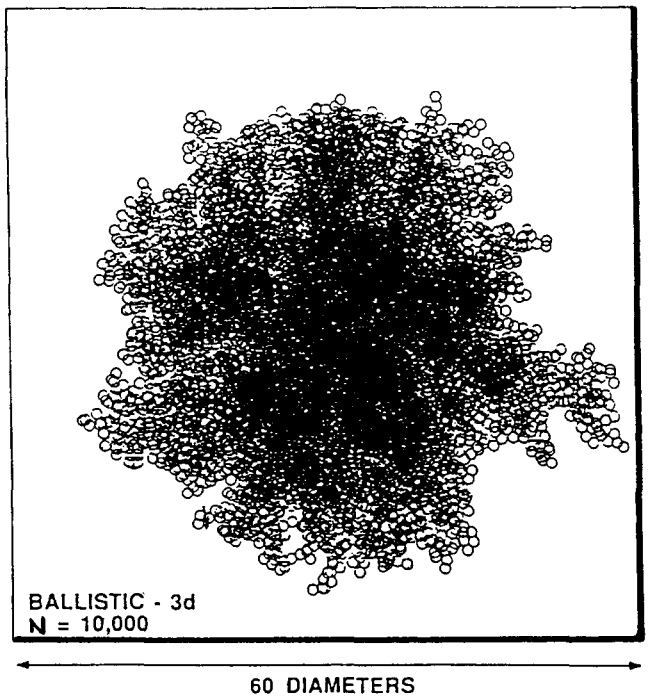

Figure 1. Simulated cluster-monomer ballistically grown three-dimensional aggregate containing 10^4 primary particles.

(After P. Meakin, as reported in Schaefer et al., 1988) ($D_f \approx 2.5$).

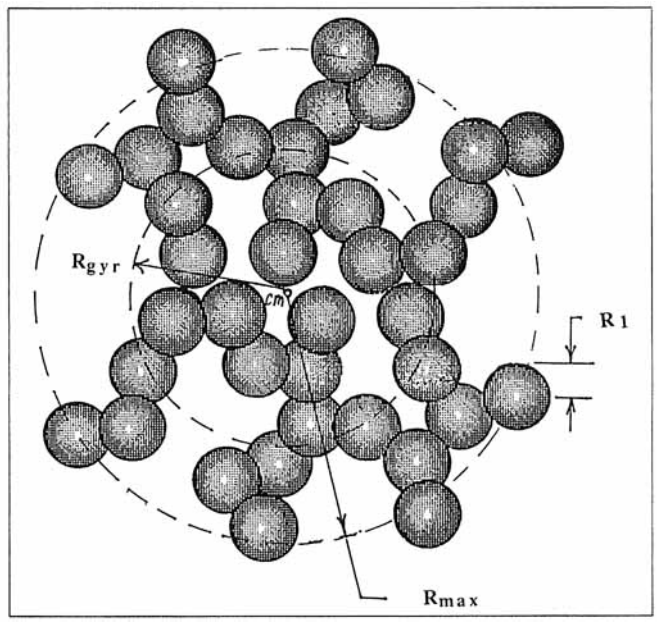

Figure 2. Mathematical model of a quasi-spherical aggregate comprised of *N*-primary spherules showing the important characteristic radii: R_1 (primary particle), R_{gyr} (aggregate), and R_{max} (characteristic aggregate outer radius (Eq. 4)).

1991; Mackowski, 1990, 1994), however, this approach becomes tedious and error-prone for *random* aggregates comprised of rather more particles, perhaps $10^2 < N < 10^6$, as have been observed in *coagulation-aged* systems. It is precisely for populations containing very large aggregates in high-pressure gases or liquids that the above mentioned shielding effects of exterior particles is expected to become appreciable, reducing their *accessible* surface area well below that of the sum of all the primary particles present.

By viewing each large quasi-spherical aggregate as a porous reactive object with a suitable radial variation of effective (pseudo-homogeneous) rate constant and effective reagent diffusion coefficient we seek and provide convenient results for the *accessible area* of large aggregates, suitable for future calculations of mass transfer between populations of such aggregates and the coexisting carrier fluid, here assumed to be a vapor mixture with non-negligible molecular mean-free-path. The general problem is shown to be conceptually identical to that of predicting the effectiveness factor of much larger solid catalyst (support) pellets in a fixed-bed chemical reactor (Aris, 1975; Butt, 1980; Satterfield, 1970; Rosner, 1986, 1990) except that we must now also embrace the possibility of quasi-spherical aggregates that are so sparse as to be essentially transparent to probing molecules traveling on straight line (balllistic) trajectories. Each class of possibilities is conveniently characterized by the so-called *fractal dimension* or *scaling exponent*, D_f, defined by $d \ln N / d \ln r$, where N is the number of primary particles contained in an imaginary sphere of radius r drawn about the aggregate center of mass (Figure 2) (Meakin, 1983; Mountain et al., 1984; Dobbins et al., 1987; Schmidt-Ott et al., 1988a, 1990). In the absence of aggregate restructuring, D_f has been observed to be about 1.8 in a wide variety of systems (physically or optically sampled, as well as computer-simulations of aggregate-aggregate encounters), but probably because of partial restructuring, aggregates have been reported with intermediate D_f-values, for example, 2.18 for the silver aggregates experimentally studied by Schmidt-Ott et al. (1988). The value $D_f = 2.5$ has recently been reported for the metal oxides produced by spray precipitation-oxidation in the seeded premixed flame experiments of Matsoukas and Friedlander (1991). In this classification scheme complete restructuring (but without true fusion, which would ultimately obliterate evidence of the primary spheres) is, of course, equivalent to the familiar limiting case $D_f = 3$, corresponding to radially constant properties and a sharply defined outer radius $R_{max}(N)$ larger than the gyration radius R_{gyr} by the familiar factor $(5/2)^{1/2}$, as, for example, in a small virgin charcoal or polycrystalline graphite particle (Dixon-Lewis et al., 1991). [Some authors (for example, Ulrich, 1984) distinguish between physically bound aggregates (easily broken apart) and partially fusion-bonded agglomerates, but this particular distinction will not concern us here.] The goal of the present analysis can then be concisely stated as follows: For a specified aggregate (N, D_f) composed of a large number N of primary spheres of (nearly) uniform radius R_1, on the surface of which a first-order rate process occurs with reaction probability α, in an environment characterized by the mean-free path l_g, what is the ratio of the effective (accessible) surface area to the sum of the primary sphere surface areas? We seek a rational, yet convenient set of quantitative relationships which will permit such calculations over the spectrum of carrier fluid mean free-paths from values so small that continuum (bulk) diffusion occurs even with the gas-filled "pores," to values large enough to not only

lead to Knudsen diffusion within the pores but to also reduce the diffusional resistance of the external fluid layer surrounding the aggregate. The procedures we ultimately recommend are efficient enough to be used to predict the accessible area and transport behavior of *populations* of such aggregates but such applications (Rosner and Tandon, 1993a) are beyond the scope of this article. Some of our methods and results would also be applicable to microporous catalyst supports in fixed-bed reactors, to which Sheintuch and Brandon (1989) have recently applied similar pseudo-continuum methods. These authors treated steady and nonsteady $D_f \geq 2.4$ cases in the absence of external diffusion limitations or noncontinuum (gas kinetic) effects. In the formulation which follows we explicitly deal with a suspended quasi-spherical aggregate comprised of a large number (N) of primary spheres, and develop a convenient rational correlation for our effectiveness factor results in terms of the prevailing reaction probability α, Knudsen number based on primary sphere diameter, Kn_{2R_1}, and the number of primary spheres in the aggregate over a broad range of observed fractal dimensions, D_f.

We present a self-consistent, tractable pseudo-continuum mathematical model for computing the accessible area of a large quasi-spherical fractal aggregate, including the radial distributions of effective pseudo-homogeneous rate constant and reactant molecule effective diffusivity. An efficient finite-analytic method is implemented for the required numerical integrations, and a convenient correlation procedure is developed based on the introduction of an effective Thiele modulus and the well-known relationship valid for the limiting case $D_f = 3$. Results for three particular D_f-values (2.5, 2.18, 1.8) in both Knudsen number limits are discussed as well as those which account for arbitrary Kn and external transport limitations. Tests of the recommended effective Thiele modulus correlation procedure for η_{int} are included. Our principal assumptions and approximations are briefly defended, and several validity criteria and tractable generalizations of current interest are described. Finally, our recommended predictive procedure and its application to coagulation-aged *aggregate populations* are summarized.

Mathematical Model

Basic assumptions

To capture the essential features of simultaneous diffusion and surface reaction in a large aggregate comprised of many ($N \gg 1$) spherical primary particles, our idealized mathematical model is based on the following underlying assumptions:

(A1) The aggregate behaves like a motionless quasi-spherical "porous" granular solid with position-dependent *area per unit volume,* a''', and effective diffusivity for reactant molecules, $D_{A,\text{eff}}$.

(A2) The radial dependence of the effective first-order rate constant and effective diffusivity for reactant molecules are dictated by the aggregate (fractal) exponent D_f defined by $d\ln N/d\ln r$ (see the second section for details).

(A3) A first-order chemical (or physical) process occurs on the external surface of each dense primary spherical particle comprising the aggregate and negligible area is lost at the primary particle contact points. [The second part of this assumption must ultimately be abandoned with the growth of strong fusion bonds between primary particles (see Koch and Friedlander, 1990, for a recent summary of this rate process), or loss of area as a result of extensive capillary condensation or growth (CVD) from the vapor.]

(A4) Reagent A, of small size compared to the primary particles, is steadily supplied to the intrinsic surfaces of the aggregate by radial diffusion through the gas-filled tortuous pores defined by the void space between the primary particles.

(A5) The aggregate may be approximated as isothermal, that is, each primary particle is at nearly the same steady-state temperature regardless of its position within the aggregate (see, also, the section discussing primary sphere surface roughness).

(A6) When the gas mean-free-path is negligible compared to R_{max}, radial concentration diffusion of reagent also occurs throughout the space $R_{max} \leq r \leq \infty$ *external* to the aggregate, where it is not appreciably impeded by the presence of primary particles.

We postpone to the fourth section a defence of these idealizations, and provide criteria to define their approximate limits of validity. Several will be seen in the fifth section to be readily generalized to embrace more complex situations that will undoubtedly arise in particular applications. Tentative secondary assumptions introduced to illustrate our *procedures* (for example, the nature of the tortuosity-void fraction relation for Knudsen- or bulk-diffusion) will be introduced, as required, to proceed.

Aggregate structure for $D_f \leq 3$

For an aggregate whose $N(r)$ relation is of the power-law form: $N \sim \beta(r/R_1)^{D_f}$, where β is a dimensionless constant discussed below, we have the basic relation:

$$dN = \beta D_f \left(\frac{r}{R_1}\right)^{D_f - 1} \cdot \frac{dr}{R_1} \tag{1}$$

describing the (expected) number of primary particles within a shell of thickness dr located at radius r (see Figure 2). [This level of description, in which Eq. 1, in effect, defines an ensemble-averaged radial distribution function for these spatially nonuniform random structures, will prove adequate to our present needs. However, in developing theories of the *restructuring kinetics* of such aggregates (see last section) additional microstructural information *is* needed, and we introduce and track the evolution of the *pdf* of angles between triplets of contacting primary particles (Cohen and Rosner, 1994).] This, in turn, implies that the *local solid fraction,* $\phi\{r\}$, is given by:

$$\phi\{r\} \equiv 1 - \epsilon\{r\} = \frac{\beta D_f}{3} \cdot \left(\frac{r}{R_1}\right)^{-(3 - D_f)} \tag{2}$$

We now note that when $D_f \to 3$, $\phi \to \beta = \text{const.}$ so that the dimensionless factor β (sometimes called the "filling factor") may be identified with the value of the solid fraction in the uniform porosity limit; that is, $\beta = \phi_{\lim} = 1 - \epsilon_{\lim}$, which, for a random loose packing of uniform size impenetrable spheres, will be about 0.6. Indeed, we visualize that, in general, Eq. 1 applies only outside of a uniform porosity "core" of radius R_c, where:

$$\frac{R_c}{R_1}=\left(\frac{\beta D_f}{3}\cdot\frac{1}{1-\epsilon_{\lim}}\right)^{1/(3-D_f)} \tag{3}$$

This equation indicates that the core radius is necessarily of order R_1, that is, quite small on the scale of the overall aggregate size defined more sharply below.

Whereas most aggregate research has focused attention of the *radius of gyration*, R_{gyr}, we instead introduce the *effective outer radius*, R_{max}, defined by:

$$R_{max}\equiv\left[\frac{3}{2}\left(\frac{D_f+2}{D_f}\right)\right]^{1/2}\cdot R_{gyr} \tag{4}$$

which is seen to reduce to the true outer radius of the spherical aggregate in the $D_f\to 3$ (uniform porosity) limit. [R_{gyr} is defined such that the actual rotational moment of inertia of the sphere is the same as if all of its mass were concentrated at its gyration radius. Rogak and Flagan (1990), who were primarily concerned with estimating aggregate particle *drag* in the creeping flow continuum limit, introduce an outer radius similar to that given in Eq. 4 but omitting the factor $(3/2)^{1/2}$. In view of the nature of the $D_f\to 3$ limit we recommend Eq. 4 in such future studies. Mulholland et al. (1988) suggested that the *collision radius* of free-molecule clusters (with $D_f=2$) is about 21% greater than R_{gyr}. Note that $\{(3/2)[(2+2)/2]\}^{1/2}=\{(3/2)\cdot(2)\}^{1/2}=1.73$. Thus, the effective collision radius appears to be somewhat less than R_{max}, which is expected on physical (partial penetration) grounds.] Beyond $r=R_{max}$ we treat the domain as primary particle-"free," at least insofar as perimeter-averaged reagent radial diffusion is concerned—that is, we treat $r=R_{max}$ as though it were a "sharp" boundary of the large N aggregate (Figure 2).

Summarizing, if we define the normalized radial variable $\zeta\equiv r/R_{max}$, our idealized model of a large quasi-spherical aggregate containing N primary particles is as follows:

$$\epsilon=\epsilon_{\lim}\approx 0.4 \quad \text{for } (0\le\zeta\le\zeta_c\ll 1) \tag{5a}$$

$$\epsilon\{\zeta\}\approx 1-\frac{\beta D_f}{3}\cdot\left(\frac{N}{\beta}\right)^{-(3-D_f)/D_f}\cdot\zeta^{-(3-D_f)} \quad \text{for } (\zeta_c<\zeta\le 1) \tag{5b}$$

$$\epsilon=1 \quad \text{for } (1\le\zeta<\infty) \tag{5c}$$

where ϵ is the familiar *void fraction* or *porosity*, $1-\phi\{\zeta\}$, and $\beta=\phi_{\lim}\approx 0.6$. Whereas higher-order microstructural information (see, for example, Torquato, 1991, or Tassopoulos and Rosner, 1991, 1992) may be needed to increase the accuracy of our Knudsen diffusion coefficient estimates (below), for our present purposes the above level of information will prove to be sufficient—as discussed in the next two subsections.

Bulk diffusion and Knudsen diffusion laws: associated tortuosities

For reagent A diffusion within the aggregate void space we must distinguish between two limiting cases depending upon the ratio of the mean-free-path l_A, to the local mean pore diameter. When this ratio (the local pore Knudsen number) is very small we write:

$$D_{A,\text{eff}}=(\epsilon/\tau_c\{\epsilon\})\cdot D_{A\text{-mix}} \tag{6}$$

where $D_{A\text{-mix}}$ is the ordinary Fick diffusion coefficient for species A migration within the prevailing gas mixture and $\tau_c(\epsilon)$ is the continuum-limit tortuosity of the local pore structure with void fraction ϵ. Similarly, in the opposite limit ($Kn_{\text{pore}}\gg 1$) we write:

$$D_{A,\text{eff}}=(\epsilon/\tau_K\{\epsilon\})\cdot D_K \tag{7}$$

where D_K, the Knudsen diffusion coefficient for species A migration down a single straight pore of uniform diameter, is given (for diffuse scattering) by:

$$D_K=(1/3)\bar{c}_A\cdot\{(2/3)[\epsilon/(1-\epsilon)](2R_1)\} \tag{8}$$

[Otherwise D_K should contain an additional factor $(2-f)/f$, where f describes the fraction of scattering events which are "diffuse" (cf. "specular").] Here $\bar{c}_A$ is the mean thermal speed of gas molecule A and the bracketed factor is the mean pore diameter for a random packing of impenetrable spheres of radius R_1 and void fraction ϵ. While recent research (for example, Tassopoulos and Rosner, 1992; Melkote and Jensen, 1992) has indicated that the Knudsen transition is probably somewhat more complex, for arbitrary Kn_{pore} we here adopt the familiar additive resistance relation:

$$D_{A,\text{eff}}=\epsilon\cdot\left\{\frac{\tau_c\{\epsilon,\ldots\}}{D_{A\text{-mix}}}+\frac{\tau_K\{\epsilon,\ldots\}}{D_K}\right\}^{-1} \tag{9}$$

(see, for example, Butt, 1980), which correctly recovers the above mentioned limiting formulae, Eqs. 6 and 7. It remains for us to specify the indicated continuum and Knudsen tortuosities for the random packing of impenetrable spheres encountered in such self-similar quasi-spherical aggregates as depicted in Figures 1 and 2.

Recent research has shown that $\tau_c(\epsilon)$ is *microstructure-insensitive* and often adequately described by a power-law in ϵ (Tassopoulos and Rosner, 1992). Imposing the limits $\tau_c\{1\}=1$ and $\tau_c\{0.4\}=1.48$ (Huizenga and Smith, 1986), we therefore tentatively adopt (irrespective of D_f):

$$\tau_c\{\epsilon,\ldots\}\approx\epsilon^{-0.416} \tag{10}$$

Knudsen regime tortuosities $\tau_K\{\epsilon\}$ are known to be more *microstructure-sensitive*, and vary more nearly linearly with the local void fraction ϵ (Tassopoulos and Rosner, 1992). [Elias-Kohav et al. (1991) have recently calculated the tortuosity-porosity relation for a variety of two-dimensional fractal porous media and contrasted them to the behavior of fully random objects. In our future work we plan to probe τ for computer-generated three-dimensional aggregates (cf. the analogous work of Tassopoulos and Rosner (1991) on planar granular deposits.] Imposing the limits: $\tau_K\{1\}=1$, and $\tau_K\{0.4\}\approx 1.86$ (Olague et al., 1988), we therefore tentatively adopt (irrespective of D_f):

$$\tau_K\{\epsilon\}\approx 1.86-1.433(\epsilon-0.40) \tag{11}$$

While the *methods* developed below will readily allow the introduction of more complex tortuosity laws should they prove necessary, all specific illustrations contained below (results and

discussion section) will be based on these particular relations for the determination of $D_{A,\text{eff}}\{r\}$.

First-order irreversible sink law for k'''_{eff}

Consider a first-order rate process occurring on the external surface of each primary particle. For a collection of such spheres the available *surface area per unit volume, a'''*, can be written:

$$a''' = 3\phi\{r\}/R_1 \tag{12}$$

where $\phi(r)$ is the above mentioned local solid fraction. Therefore, the pseudo-homogeneous rate constant k'''_{eff} will be taken to be:

$$k'''_{\text{eff}} = k''_{\text{eff}}\, a''' \tag{13}$$

From a kinetic theory viewpoint k''_{eff}, the *heterogeneous* rate constant (velocity) can be reexpressed:

$$k''_{\text{eff}} = (1/4)\alpha\bar{c}_A \tag{14}$$

where α is the dimensionless reaction probability ($\alpha \le 1$) and $\bar{c}_A$ is again the mean thermal speed of species A. [This type of kinetic law can also be used to describe physical *condensation* (with condensation probability α) or *evaporation*, with evaporation sublimation coefficient α, to be discussed later.] While α is not really an elementary rate constant (Rosner, 1972), for our present purposes we will treat α as a specifiable parameter.

Pseudo-homogeneous reaction-diffusion model: spherical symmetry

Using the above information it is possible to derive a simple ODE for the steady-state concentration profile $n_A\{r\}$ established within the aggregate, viewing the latter as a porous sphere with known $D_{A,\text{eff}}\{r\}$ and $k'''_{\text{eff}}\{r\}$-profiles. For example, a species A mass balance for a spherical shell of volume $4\pi r^2\Delta r$ located at radius r (after division by $4\pi r^2\Delta r$ and passing to the limit $\Delta r \to 0$) yields the familiar linear second-order ODE:

$$\frac{1}{r^2}\cdot\frac{d}{dr}\left[r^2 D_{A,\text{eff}}\{r\}\cdot\frac{dn_A}{dr}\right] = k'''_{\text{eff}}\{r\}\, n_A\{r\} \tag{15}$$

Introducing the normalized variables:

$$c \equiv n_A\{r\}/n_A\{R_{\max}\}, \quad \zeta \equiv r/R_{\max}, \tag{16a,b}$$

then Eq. 15 can be rewritten in dimensionless form:

$$\frac{1}{\zeta^2}\frac{d}{d\zeta}\left[\zeta^2\tilde{D}\{\zeta\}\frac{dc}{d\zeta}\right] = \Phi^2\tilde{k}c \tag{17}$$

involving the coefficient functions:

$$\tilde{D} \equiv D_{A,\text{eff}}\{r\}/D_{A,\text{eff}}\{R_{\max}\} \quad \tilde{k} \equiv k'''_{\text{eff}}\{r\}/k'''_{\text{eff}}\{R_{\max}\} \tag{18a,b}$$

and the parameter Φ, the familiar *Thiele modulus*, given explicitly by:

$$\Phi \equiv \frac{R_{\max}}{\left[\dfrac{D_{A,\text{eff}}\{R_{\max}\}}{k'''\{R_{\max}\}}\right]^{1/2}} \tag{19}$$

It is helpful to view Φ as the ratio of the aggregate radius $R_{\max}$ to the characteristic penetration depth defined by the denominator of Eq. 19. Alternatively, the parameter Φ^2 appearing on the righthand side of Eq. 17 may be regarded as the relevant *Damköhler group*—that is, the ratio of the diffusion *time* $R^2_{\max}/D_{A,\text{eff}}\{R_{\max}\}$ to the reaction *time*: $(k'''_{\text{eff}}\{R_{\max}\})^{-1}$ (Rosner, 1986, 1990, Chapter 8). Thus, once the coefficient functions $\tilde{D}\{\zeta\}$ and $\tilde{k}\{\zeta\}$ and the parameter Φ are specified, it is straightforward to find $c\{\zeta\}$ satisfying the ODE (Eq. 17) and the "split" boundary conditions:

$$c\{1\} = 1 \quad \text{and} \quad (dc/d\zeta)_{\zeta=0} = 0 \tag{20a,b}$$

(See sections on finite-analytic method and inclusion of external boundary layer limitations.) The first of these BCs follows from the definition of c (Eq. 16a); the second follows from the nonsingular behavior of the medium as $r \to 0$, (that is, within the constant porosity inner core), not exclusively "symmetry" (see Rosner, 1986, 1990, Section 6.4.4).

Definition and calculation of the "internal" effectiveness factor

Solution to the boundary value problem (BVP) defined in the previous subsection allows calculation of the single quantity of greatest interest, namely, the actual reaction rate within the aggregate compared to what it would have been had the reagent concentration remained undepleted everywhere within the aggregate. This quantity, hereafter written η_{int}, can also be regarded as the ratio of the effective (or accessible) surface area to the true total primary particle surface area within the aggregate (that is, the sum of the primary sphere areas, Na_1). For this reason this quantity is traditionally referred to as the internal effectiveness factor.

From its definition, we readily find that η_{int} can be calculated from $c\{\zeta\}$ via:

$$\eta_{\text{int}} = \frac{3}{\Phi^2}\cdot\left(\frac{dc}{d\zeta}\right)_{\zeta=1}\cdot\left\{3\int_0^1 \tilde{k}\{\zeta\}\zeta^2 d\zeta\right\}^{-1} \tag{21}$$

Thus, once the solution $c\{\zeta\}$ is obtained (see next subsection) the internal effectiveness factor (or normalized accessible area) is readily found from Eq. 21. It is interesting to note that since the core radius makes a negligible contribution to this indicated integral, Eqs. 2, 13, 18, and 21 imply that:

$$\eta_{\text{int}} \approx (D_f/\Phi^2)\cdot(dc/d\zeta)_{\zeta=1} \quad (D_f \le 3) \tag{22}$$

which is a straightforward generalization of the familiar $D_f = 3$ (constant porosity) result (cf., for example, Rosner, 1986, 1990). However, in developing a compact correlation for all of our computed results, Eq. 21 will prove to be more illuminating (see subsection after next).

Finite-analytic method

While most transport (boundary value) problems do not have

analytic solutions, some, like ODE (Eq. 17) and its BCs, admit analytic solutions if the coefficient functions are assumed to be constant [here $\tilde{k}\{\zeta\}$ and $\tilde{D}\{\zeta\}$]. In such situations, an attractive scheme to solve the problem is to simply divide the domain into sublayers, each with *piecewise-constant* local coefficients. The BVP over the whole domain can then be solved by applying appropriate continuity conditions at the boundaries of each sublayer. Because we use local analytic solutions applicable within each sublayer this variant of the finite-difference method has been assigned the name: "finite-analytic" method (Chen and Chen, 1984; Rosner et al., 1987; and Rosner, 1986, 1990, p. 484). For any fixed number of sublayers we expect the error involved to be considerably less than that involved in direct discretization of the governing differential equation(s). The finite-analytic approach thus facilitates rapid convergence to the exact solution, allowing division of the domain into fewer sublayers. What follows is a brief account of its implementation for the problem at hand.

For constant $\tilde{D}$ and $\tilde{k}$, the exact solution to Eq. 17 takes the form:

$$c = [A \exp\{a\zeta\} + B \exp\{-a\zeta\}]/\zeta \tag{23}$$

where $a \equiv (\tilde{k}/\tilde{D})^{1/2}\Phi$.

With the boundary conditions @ $\zeta = \hat{\zeta}_1$ $C = \hat{c}_1$ and $\zeta = \hat{\zeta}_2$ $C = \hat{c}_2$, the constants A and B are:

$$A = [\hat{c}_1 \hat{\zeta}_1 \cdot \exp\{a\hat{\zeta}_1\} - \hat{c}_2 \hat{\zeta}_2 \cdot \exp\{a\hat{\zeta}_2\}]/[\exp\{2a\hat{\zeta}_1\} - \exp\{2a\hat{\zeta}_2\}]$$

$$B = [\hat{c}_1 \hat{\zeta}_1 \cdot \exp\{a\hat{\zeta}_1\} - \hat{c}_2 \hat{\zeta}_2 \cdot \exp\{-a\hat{\zeta}_2\}]/[\exp\{-2a\hat{\zeta}_1\} - \exp\{-2a\hat{\zeta}_2\}] \tag{24}$$

and

$$dc/d\zeta = [A \exp\{a\zeta\}(a\zeta - 1) - B \exp\{-a\zeta\}(a\zeta + 1)]/\zeta^2$$

For a porous medium with fractal exponent $D_f < 3$, the coefficient functions $\tilde{D}$ and $\tilde{k}$ are not constant and depend on ζ through the local porosity $\epsilon\{\zeta\}$ of the medium, as discussed earlier. Thus, to solve the problem of diffusion and reaction in the "fractal" aggregate we assume that the porous medium consists of a central core with constant porosity enveloped by successive concentric annular shells. The porosity (and therefore $\tilde{k}$ and $\tilde{D}$) is assumed to be constant within each of these shells but differs from shell to shell (in accord with ϵ evaluated at each shell arithmetic mean radius), as given by Eq. 5. The analytic solution as given by Eq. 23 holds within each of these shells for the local values of $\tilde{k}$ and $\tilde{D}$. As illustrated in Figure 3, the outer region has been divided into n zones (shells) and $n+1$ nodes. Defining c_i and ζ_i as dimensionless concentration and distance from center at node i, respectively, (cf. Figure 3a) the following condition should be satisfied at each node i:

$$\left(\tilde{D}\left(\frac{dc}{d\zeta}\right)_{\zeta=\zeta_i}\right)_{\text{zone}=i-1} = \left(\tilde{D}\left(\frac{dc}{d\zeta}\right)_{\zeta=\zeta_i}\right)_{\text{zone}=i} \tag{25}$$

Substituting from Eqs. 23 and 24 we get a linear algebraic relationship between c_{i-1}, c_i, and c_{i+1}. Writing Eq. 25 for $i = 2$, 3, ... n we have $n-1$ linear algebraic equations in $n+1$ variables (c_i, $i = 1, .. n+1$). The two other required equations are:

$$c_{n+1} = 1 \tag{26}$$

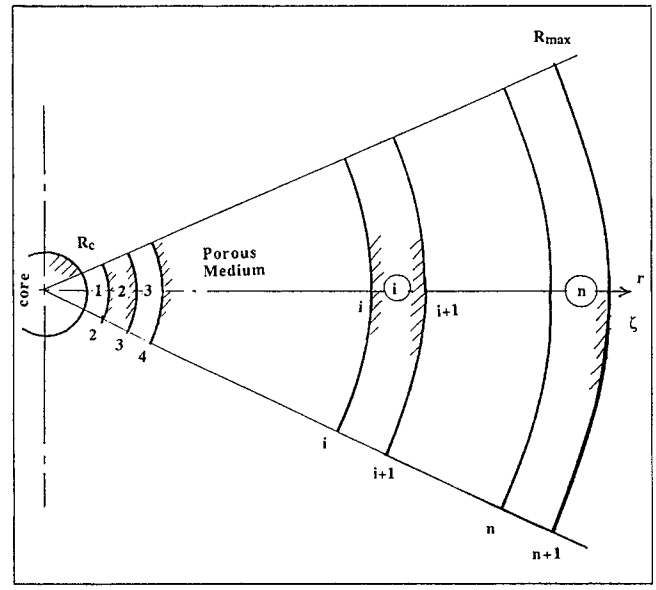

Figure 3a. Discretization nomenclature for implementation of a finite-analytic method (FAM) to solve numerically the present radial diffusion/pseudohomogeneous reaction model for the accessible area of a large, quasi-spherical multiparticle aggregate of nonuniform porosity.

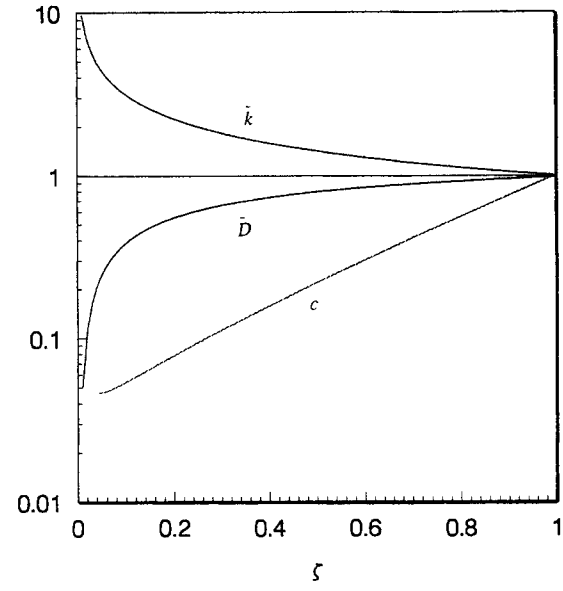

Figure 3b. Typical radial profiles of normalized pseudohomogeneous reaction rate coefficient ($\tilde{k}$), reagent diffusion coefficient ($\tilde{D}$), and corresponding steady-state normalized composition profile (c).

Logarithmic ordinate; case shown: $D_f = 2.5$, $N = 10^5$, $\alpha = 10^{-1}$, and $Kn_{2R_1} = 10$.

and species A flux continuity condition at $\zeta = \zeta_{core}$.

$$\left(\tilde{D}\left(\frac{dc}{d\zeta}\right)_{\zeta=\zeta_{core}}\right)_{core} = \left(\tilde{D}\left(\frac{dc}{d\zeta}\right)_{\zeta=\zeta_{core}}\right)_{zone=1} \tag{27}$$

Inside the core the concentration profile is again given by Eq. 23 with the following boundary conditions:

$$c = c_1 \quad @ \ \zeta = \zeta_{core} \tag{28}$$

$$(dc/d\zeta)_{\zeta=0} = 0$$

From Eqs. 23 and 28 we obtain:

$$c = c_1 \sinh\{\Phi_{core}\zeta\}/(\zeta \sinh\{\Phi_{core}\}) \quad (0 \le \zeta \le \zeta_{core}) \tag{29}$$

where $\Phi_{core} = R_{core}/(D_{eff,Rcore}/k'''_{eff,Rcore})^{1/2}$.

This system of $n+1$ linear equations can be rapidly solved for the concentration profile (see, for example, Figure 3b) using Thomas' algorithm for tridiagonal matrices. The internal effectiveness factor, η_{int}, can then be calculated as Eq. 21, or, alternatively:

$$\eta_{int} = \frac{\int_0^1 \tilde{k}c\{\zeta\}\zeta^2 d\zeta}{\int_0^1 \tilde{k}\zeta^2 d\zeta} \tag{30}$$

where the indicated integrals are replaced by their equivalent algebraic sums.

In a typical $D_f = 1.8$ numerical calculation we used $n = 10$ sublayers, having determined that at even this level of subdivision our η_{int} results are quite insensitive to n. A typical Sun Sparc II station run time was less than 5 s. As a useful check on the computer program, in the special case $D_f = 3$ we recover the well known constant property result for η_{int} (see the next subsection and Figure 7).

Correlation strategy for η_{int} ($D_f \le 3$)

Despite the computational efficiency of the finite-analytic numerical method described in the previous subsection for accurately calculating η_{int} for any particular combination of the parameters N, D_f, Kn, ... and choice of laws for $\tilde{D}\{\zeta\}$ and $\tilde{k}\{\zeta\}$, it would be desirable to have available a compact, rational correlation formula which could be used to rapidly predict η_{int} with acceptable accuracy (say $< 3\%$ rms error) over the entire range of aggregate/environmental parameters of engineering interest. This is especially important for solving problems involving the presence of *populations* of aggregates, for which N covers a "spectrum" of values and we again wish to calculate the total accessible surface area per unit volume represented by this population (see second to last subsection and Rosner and Tandon, 1993a). At the outset, we should comment that while this calculation requires an overall factor $\eta_{overall}$ which is the product of η_{int} and a corresponding factor, η_{ext}, describing the effect of an external diffusion layer, we show in the next section that, once η_{int} is known it is straightforward to calculate both η_{ext} and $\eta_{overall}$ via simple explicit algebraic formulae.

Just as our finite-analytic strategy (previous subsection) for the solution of the BVP defined earlier was based on the familiar analytic behavior of the constant property ($D_f = 3$) special case, our proposed correlation for η_{int} will be based on the well-known properties of the function:

$$\eta_3\{x\} = (3/x)[(\tanh x)^{-1} - x^{-1}] \tag{31}$$

which (with $x = \Phi$) describes η_{int} in the $D_f = 3$ limit, and which behaves like $1 - (2/5)x^2 + \ldots$ for small x and $3/x$ for large x.

Inspection of the ODE (Eq. 17) suggests that when Φ is sufficiently small (to allow "deep penetration" of the reagent) the principal effect of the $D_f < 3$ terms [which lead to $\tilde{D}\{\zeta\} < 1$ and $\tilde{k}\{\zeta\} > 1$] will be to cause the solution to be similar to the $D_f = 3$ case but with an effective value of Φ "stretched" by the factor:

$$[\langle\tilde{k}\rangle/\langle\tilde{D}\rangle]^{1/2} \tag{32}$$

where $\langle\ \rangle$ is some appropriate average value of the indicated quantity over the domain $0 \le \zeta \le 1$. We postpone for the moment the question of which average is most successful and will empirically consider below members of the subclass:

$$\langle\Psi\rangle_q \equiv (1+q)\cdot\int_0^1 \Psi\{\zeta\}\cdot\zeta^q d\zeta \tag{33}$$

where Ψ is $\tilde{k}$ or $\tilde{D}$ and $q > 0$.

In the large Φ limit we know that the reagent penetration will be shallow so that $\tilde{k} = 1$ and $\tilde{D} = 1$ within this outer "boundary layer." Thus, in this limit, Eq. 21 reveals that the solution to our BVP must be:

$$\lim_{\phi \gg 1} \eta_{int} = (3/\Phi)\cdot\left\{3\int_0^1 \tilde{k}\{\zeta\}\zeta^2 d\zeta\right\}^{-1} = 3\{\langle\tilde{k}\rangle_2\Phi\}^{-1} \tag{34}$$

in which the relevant effective-Φ is seen to be "stretched" by the factor $\langle\tilde{k}\rangle_2$. Summarizing, we expect that $\eta_3\{\Phi_{eff}\}$ will be an acceptable approximation to η_{int} provided Φ_{eff} is chosen such that the stretching factor $[\langle\tilde{k}\rangle/\langle\tilde{D}\rangle]^{1/2}$ is applied for "small" Φ and the stretching factor $\langle k\rangle_2$ is applied for "large" Φ. For these reasons we simply investigate the choices:

$$\Phi_{eff}\{\Phi\} \equiv \left[\left(\frac{\langle\tilde{k}\rangle_q}{\langle\tilde{D}\rangle_q}\right)^{1/2}\right]^{1/(1+\Phi)} \cdot \Phi \cdot [\langle\tilde{k}\rangle_2]^{\Phi/1+\Phi} \tag{35}$$

For each such choice we compared values of η_{int} (correlation) with η_{int} (FAM). We found that *all* of our $D_f < 3$ η_{int}-results were quite acceptable for the choice $q = 1$. This is readily demonstrated in the "correlation" plots Figures 4, 5, and 6 for cases involving continuum (bulk) pore diffusion (Figure 4), Knudsen pore diffusion (Figure 5), and transitional Knudsen numbers (Figure 6).

One sees that the rms errors are only about 3%, with the acceptably small local errors peaking (ca. 4%) at intermediate η_{int}-values (near 0.8). Thus, to rapidly predict η_{int} for large aggregates to within about ca. 3% error one merely uses the

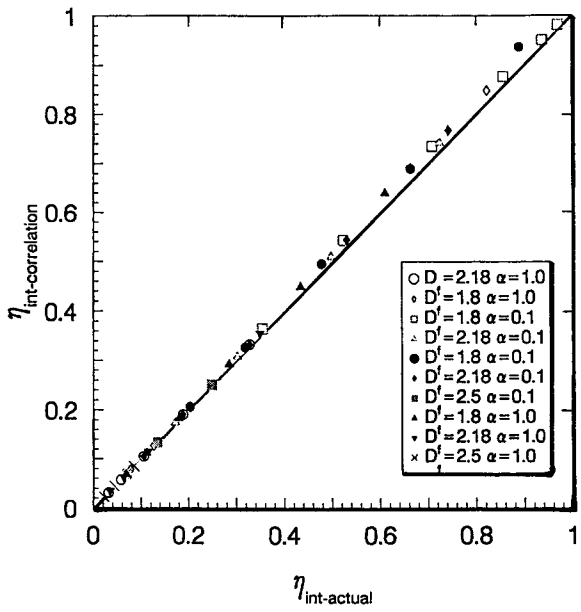

Figure 4. Test of the effective Thiele modulus correlation (Eqs. 31 and 35) for the internal effectiveness factor η_{int} of large ($N \geq 10^2$) fractal aggregates in the continuum (bulk-) pore diffusion limit.

For unshaded points $Kn_{2R_1} = 10$; for shaded points: $Kn_{2R_1} = 1$.

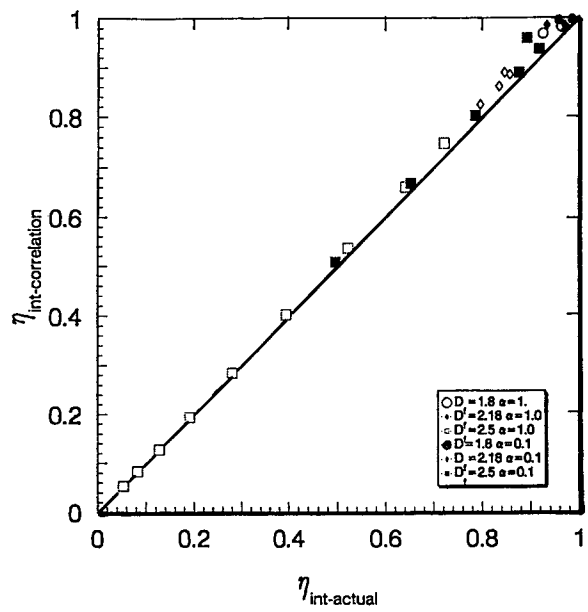

Figure 5. Test of the effective Thiele modulus correlation (Eqs. 31 and 35) for the internal effectiveness factor η_{int} of large ($N \geq 10^2$) fractal aggregates in the Knudsen pore diffusion limit.

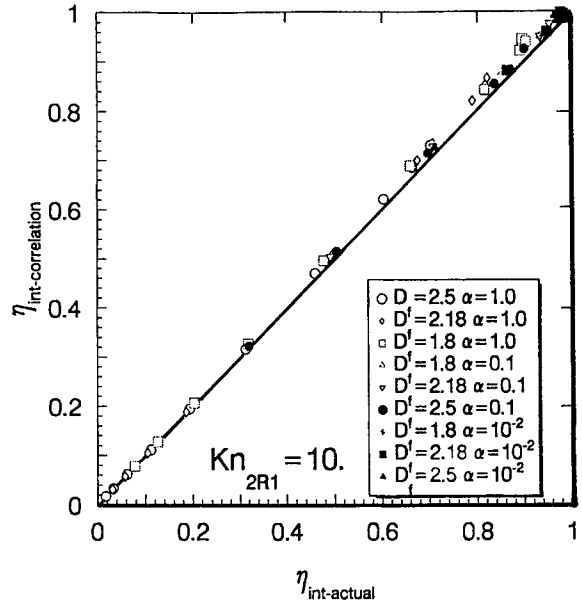

Figure 6. Test of the effective Thiele modulus correlation (Eqs. 31 and 35) for the internal effectiveness factor η_{int} of large ($N \geq 10^2$) fractal aggregates in the transition pore diffusion regime; $Kn_{2R_1} = 10$.

well-known $\eta_3\{x\}$ function with a suitably calculated (nonlinearly stretched) *effective Thiele modulus*, Φ_{eff} (Eq. 35) with $q = 1$. [We suggest that this rational correlation strategy can be implemented for a wide class of engineering problems. Earlier, closely related examples from the author's research (DER) may be found in Israel and Rosner (1983) and Rosner and Feng (1974).] Since, in this case $\langle \tilde{k} \rangle_q$ can be evaluated in closed form (for any q) this recommended procedure only requires the calculation of $\langle \tilde{D} \rangle_1$, which is a trivial numerical integration for the present class of tortuosity laws (second section), or any other choice of tortuosity laws deemed (via future research on aggregate microstructure) to be more appropriate (fourth section).

In closing this section, we remark that the acceptably small local errors of the present recommended correlation appear to be systematically positive (see Figures 4, 5, 6). This implies that a slight modification of the exponents appearing in Eq. 35 could easily reduce them further. However, the present simple version (the first we investigated!) is acceptable for our present purposes. We remark that this procedure should also be useful for estimating η_{int} for ordinary catalyst pellets ($D_f = 3$) which, because of their manufacture (pelleting, impregnation, and so on), have *spatially nonuniform* $D_{A,\text{eff}}$ and k'''_{eff} properties.

Results and Discussion

Inclusion of external boundary layer limitations

If the gas mean-free-path is small on the scale of $2R_{\max}$ (Eq. 4), then, even though the aggregate may be *internally* accessible (as when $D_f = 1.8$ and Knudsen diffusion prevails within the aggregate) the steady-state reagent concentration established at $r = R_{\max}$ will be systematically less than that in the ambient, contributing to an apparent reduction in accessible surface area. This effect of the "resistance in series" represented by the external gas boundary layer is easily included in our analysis via introduction of the additional factor:

$$\eta_{ext} = n_{A,w}/n_{A,\infty} \tag{36}$$

which is explicitly calculated below. The overall effect of internal and external diffusional resistance on the normalized accessible surface area of the aggregate will then be given by the product:

$$\eta_{overall} = \eta_{int} \cdot \eta_{ext} \tag{37}$$

where the calculation and correlation of η_{int} have already been dealt with earlier.

Our idealized mathematical model to account for the *external* diffusion layer makes use of earlier results for the dimensionless (Nusselt-Sherwood) mass-transfer coefficient for diffusional transfer to/from a motionless, isolated solid sphere, viz.

$$Nu_m = 2 \cdot \{1 + fct\{Kn\}\}^{-1} \tag{38}$$

where $Kn = l/(2R_{max})$. Note that $fct(0) = 0$ in order to recover the familiar continuum limit value 2, but $fct\{\infty\} = \infty$ to eliminate this diffusional resistance in the free-molecule limit. Several authors have calculated and/or measured the important function $fct\{Kn\}$ appearing in Eq. 38. For our present purposes we adopt the following corrected form of the Fuchs-Sutugin approximation (Friedlander, 1977):

$$fct(Kn) = 2Kn \cdot \left\{\frac{1.33 + 1.42(2Kn)^{-1}}{1 + (2Kn)^{-1}}\right\} \tag{39}$$

[The coefficient of $(2Kn)^{-1}$ in the numerator of Eq. 39 has been increased (from 0.71) to force agreement with independent $Kn \ll 1$ results.] Then a steady-state analysis in which the reagent A flow rate into the quasi-spherical aggregate is balanced against the steady-state rate of its consumption within the aggregate yields the explicit algebraic result:

$$\eta_{ext} = \left\{1 + \frac{\frac{\alpha}{4}\bar{c}_A a_1 N \cdot \eta_{int}}{2\pi R_{max} Nu_m D_{A\text{-mix}}}\right\}^{-1} \tag{40}$$

where a_1 ($= 4\pi R_1^2$) is the surface area of a primary spherule.

For the illustrative calculations given below we will assume that reagent A has a molecular mass and collision cross-section similar to that of the background gas mixture, so that $l_g = l_A$. We will also make use of the corresponding molecular theory estimate:

$$D_{A\text{-mix}} \approx (1/3) l_A \cdot \bar{c}_A \tag{41}$$

These (unnecessary) assumptions will simply reduce the number of parameters that must be specified in the examples below, and thereby help us focus on the essential trends. With these simplifications we find that $\eta_{overall}$ can be expressed:

$$\eta_{overall} \cong \left\{\frac{1}{\eta_{int}} + \frac{\frac{3}{4}\alpha\beta\left(\frac{R_{max}}{R_1}\right)^{D_f - 1}}{Nu_m \cdot Kn_{2R_1}}\right\}^{-1} \tag{42}$$

where Kn_{2R_1} is the Knudsen number based on primary sphere diameter $2R_1$, a quantity specified explicitly in the aggregate transport calculations illustrated below. Thus:

$$Kn \equiv l/(2R_{max}) = Kn_{2R_1} \cdot (R_{max}/R_1)^{-1} = Kn_{2R_1} \cdot (N/\beta)^{-1/D_f} \tag{43}$$

which fixes Kn (cf. Eq. 39) for every choice of aggregate size N and Knudsen number based on primary sphere diameter.

Illustrative results and implications

Before examining representative results for $\eta_{overall}$ it is interesting to examine the sensitivity of η_{int} to the structural exponent D_f and aggregate size N. One such set of results is shown in Figure 7, which reveals that even for a reaction probability of unity, and for aggregates containing very many primary particles, if D_f is less than 2 and Kn_{2R_1} is large enough (here $Kn_{2R_1} = 10$) essentially the entire aggregate area is "accessible" ($\eta_{int} \approx 1$). [Indeed, for $D_f < 2$ one finds that for Knudsen pore diffusion the *penetration depth* $[D_{A,eff}\{R_{max}\}/k'''_{eff}\{R_{max}\}]^{1/2}$ increases more rapidly with N than R_{max} itself, that is, the relevant Thiele modulus Φ actually *decreases* with increasing N! However, even for $D_f < 2$ this remarkable behavior does not occur in the continuum pore diffusion limit ($Kn_{pore} < 1$).] However, for a given N-value (say, $N = 10^5$) one sees that η_{int} falls off rapidly at higher values of the exponent D_f. Thus, if for any reason restructuring of an initially $D_f = 1.8$ aggregate containing N primary particles occurred, η_{int} would drop accordingly, even if primary sphere *fusion* did not occur.

In Figure 8, which serves as one check on our general computer program (incorporating the pore diffusion transition between continuum and Knudsen), we show how η_{int} relates to its (separately computed) continuum- and Knudsen-pore diffusion asymptotes. Note that, in the "small" N domain, because of the reduced average pore size, one approaches the Knudsen diffusion asymptote, whereas for $N \gg 1$ more of the aggregate pores fall in the continuum (bulk) diffusion regime.

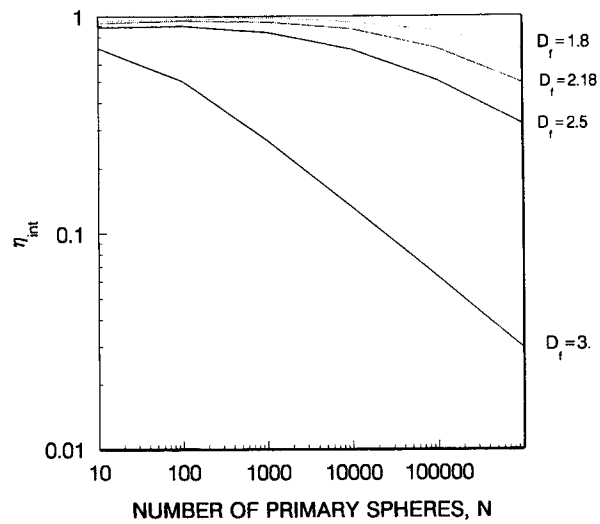

Figure 7. Predicted dependence of the internal effectiveness factor, η_{int}, on a aggregate size N and fractal dimension D_f for $\alpha = 10^{-1}$; $Kn_{2R_1} = 10$.

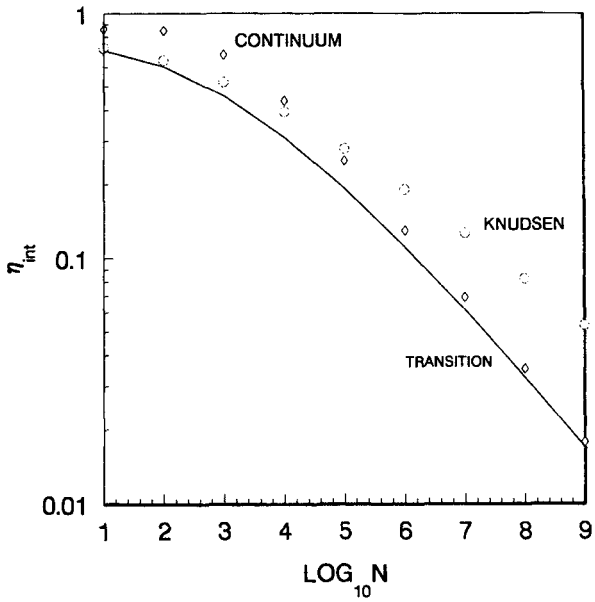

Figure 8. Nature of the η_{int} transition from obstructed continuum (bulk-) diffusion to Knudsen pore diffusion for large quasi-spherical aggregates ($D_f = 2.5$, $Kn_{2R_1} = 10$, $\alpha = 1$).

This particular graph applies to the parameter combination: $D_f = 2.5$, $\alpha = 1$, $Kn_{2R_1} = 10$. However, as commented above, even for $D_f = 1.8$ low values of η_{int} result at small enough ambient mean free paths (high enough pressures).

For the same value of Kn_{2R_1} Figures 9 and 10 reveal the sensitivity of the overall normalized accessible surface area, $\eta_{overall}$, to aggregate size N and reaction (or "trapping") probability α, for the important special cases $D_f = 1.8$ (open aggregates) and $D_f = 2.5$ (more compact aggregates). We remark that the exponent $D_f = 1.8$ (± 0.1) has been observed or inferred for aggregate smokes in many combustion environments (see

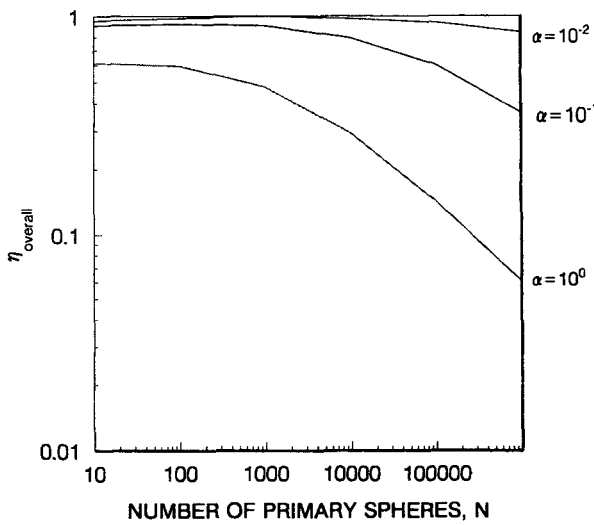

Figure 9. Predicted dependence of the overall effectiveness factor, $\eta_{overall}$, on aggregate size N and reaction probability α for $D_f = 1.8$ ($Kn_{2R_1} = 10$).

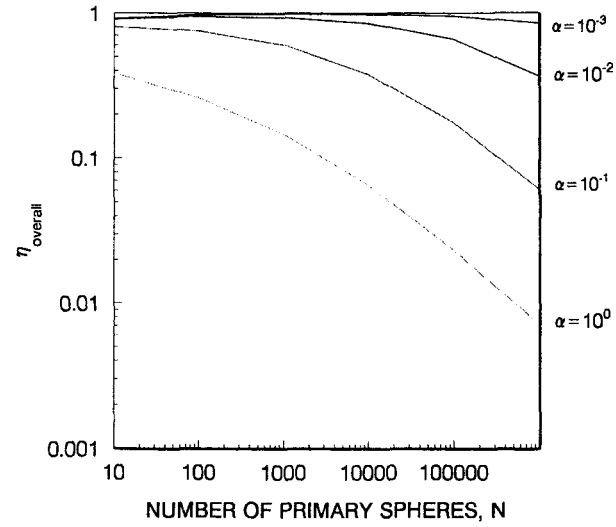

Figure 10. Predicted dependence of the overall effectiveness factor, $\eta_{overall}$, on aggregate size N and reaction probability α for $D_f = 2.5$ ($Kn_{2R_1} = 10$).

the useful summaries of Megaridis and Dobbins (1990) and Puri et al. (1993). [Megaridis and Dobbins (1990) have also called attention to the narrow size *range* (spread) of the primary particle diameters in particular laminar flow environments. Primary particle diameters reported are often of the order of tens of nanometers, which accounts for the very high specific surface areas of these materials.] The value $D_f = 2.5$ was recently observed for aggregated metal oxide smokes produced by spray pyrolysis-oxidation of aqueous metal salts in laminar, atmospheric pressure premixed flames (Matsoukas and Friedlander, 1991). Monte Carlo simulation studies in 3 dimensions (Meakin, 1983, 1984) reveal that the D_f-values near 1.8 result from cluster-cluster agglomeration whereas D_f-values near 2.5

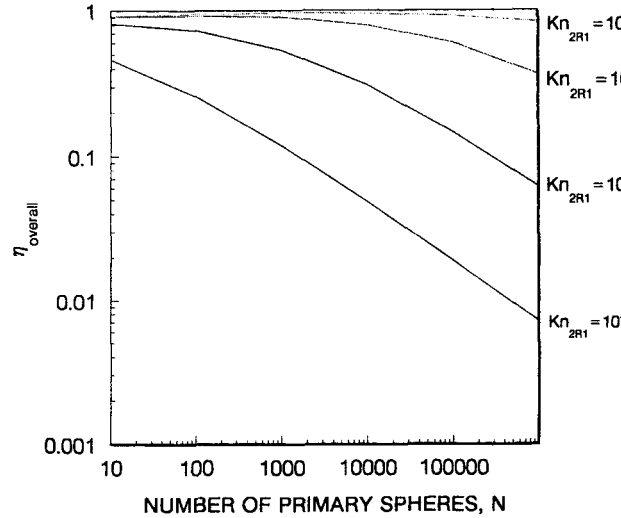

Figure 11. Predicted dependence of the overall effectiveness factor, $\eta_{overall}$, on aggregate size N and gas mean free path (in multiples of $2R_1$) for a reaction probability α of 10^{-1} ($D_f = 1.8$).

result from cluster-monomer aggregation in the absence of further restructuring (Figure 1). Whatever the prevailing D_f-value, our procedure is seen to facilitate rational predictions of the accessible surface area of large quasi-spherical aggregates as a function of both reaction probability and Knudsen number.

Whereas some authors have stated or implied that aggregates with $D_f \leq 2$ are always "totally accessible" this will clearly *not* be the case at pressure levels large enough to cause the mean-free-path to be comparable with the average pore diameter $\{(2/3)[\epsilon/(1-\epsilon)](2R_1)\}$, or, certainly, the primary particle diameter. Moreover, unless l_g is large compared to $2R_{max}$, the external boundary layer limitation is not escapable. This is clearly illustrated in Figure 11 for the case of $D_f = 1.8$ with a reaction probability of 10^{-1}. We remark that reaction probabilities of approximately this order of magnitude have been reported for the *oxidation* of suspended carbonaceous soot by OH(g) or O(g) (Neoh et al., 1981; Roth et al., 1990). In contrast, inferred reaction probabilities for the growth of "young" soot via C_2H_2(g) impacts are of the order of 10^{-3} (Harris and Weiner, 1984). Our approach and results may therefore be of special interest in high-pressure devices—such as modern aircraft gas turbine combustors (which operate at ca. 30 atm, Correa and Shyy, 1987), or flame-produced TiO_2(s) (chloride-process) pigment reactors (Ulrich, 1984). In this respect, re-examination of Eq. 41 used above indicates that, provided assumptions 1-6 (second section) are satisfied, our present results could also be used to estimate the accessible area of such aggregates in supercritical vapors (Mohamed et al., 1989) or true liquids (Matijevic, 1981; Zukoski et al., 1990) by setting $Nu_m = 2$, and reinterpreting Kn_{2R_1} as a dimensionless solute diffusion coefficient (inverse Peclet number):

$$Kn_{2R_1} = (D_{A\text{-mix}})_{exp}/\{((1/3)\bar{c}_A)\cdot(2R_1)\} \tag{44}$$

where $(D_{A\text{-mix}})_{exp}$ is the experimental solute A Fick (or Brownian-) diffusion coefficient in the prevailing fluid, and the mean molecular speed $\bar{c}_A$ is formally calculated using gas kinetic theory. In this respect the effective reaction probability, α_{eff}, should be calculated from:

$$\alpha_{eff} = (k'')_{exp}/[(1/4)\bar{c}_A] \tag{45}$$

Clearly, however, these results would have to be generalized to deal with ("hindered" diffusion) situations in which the effective size of a (macro-) solute A is not negligible compared to the prevailing spherule diameter (cf. A4). Indeed, Hagenlock and Friedlander (1989) have carried out Monte Carlo simulations of finite size gas molecules striking $D_f = 2.5$ aggregates of spheres with $N \leq 10^3$, keeping track of collision frequency (assuming diffuse reflection) as a function of aggregate size and gaseous Knudsen number $l_g/(2R_1)$. Remarkably, they report steady-state collision frequencies less than that expected for N isolated spheres even in the *nonreactive* limit ($\alpha \to 0$) and point molecule limit ($\sigma_A/(2R_1) \to 0$), a paradoxical result evidently at variance with the predictions of our present pseudo-continuum model (for which $\eta_{int} \to 1$ when $\alpha \to 0$ and $\sigma_A/(2R_1) \to 0$ for any fixed N, Kn).

Discussion

Equations 15-43 will clearly permit rapid estimates for many parameter combinations of particular interest to the reader. Moreover, as mentioned in the fifth section and will be explicitly illustrated in Rosner and Tandon (1993a), they are readily applied to predict the accessible area of, say, log-normal *populations* of aggregates frequently observed in coagulation-aged systems (Matsoukas and Friedlander, 1991).

It is noteworthy that, whereas Meakin and Whitten (1983), using Monte Carlo simulation methods, have implied that the accessible area (or interface) of an aggregate will scale as a simple power (near 0.74 in 3 dimensions) of the total aggregate size, our pseudo-continuum relations, which also include external boundary layer effects, reveal that the actual relationship will not be so simple. This is readily seen by examining the range of values of $1 + (d\,ln\,\eta_{overall}/d\,ln\,N)$ revealed in Figures 9, 10, and 11. (Note that the logarithmic coordinates of these figures allow direct visualization/computation of the required local logarithmic derivative.)

It is also interesting to note that the present approach can shed useful light on the meaning of recent experimental measurements suggested to characterize aggregates *in situ*. One such measurement recommended and illustrated by Schmidt-Ott (1988) is the so-called *attachment coefficient* for aggregate scavenging of, say, radioactive ^{211}Pb(g)-atoms. In our notation this quantity (called β by Schmidt-Ott) is equivalent to:

$$\beta_{S\text{-}O} = (1/4)\alpha\bar{c}_A a_1 \cdot N\,\eta_{overall} \tag{46}$$

where the important *product* $N\cdot\eta_{overall}$ may be regarded as the accessible (or "exposed") number of primary particles, and, in this case, $A \equiv {}^{211}Pb(g)$. In the near free-molecular limit ($Kn \gg 1$) this coefficient has been shown to be approximately proportional to the *photoelectron yield* (Burtscher and Schmidt-Ott, 1985) of small ($N \leq 40$, $D_f \approx 2.18$, $R_1 \approx 7.5$ nm) aggregates of silver illuminated by *uv* radiation ($\lambda \approx O\{200$ nm$\}$. [This is already an example for which l_A should be distinguished from the gas *mixture* mean-free-path, and Eq. 41 for $D_{A\text{-mix}}$ suitably generalized (Rosner, 1986, 1990).] However, inspection of Eq. 42 and the laws of *electron* scattering in gases suggests that this linearity is not likely to be preserved in the continuum (high-pressure) limit.

It is also noteworthy that there may be a sort of "Reynolds analogy" relation (Rosner, 1986) between the mass-transfer (scavenging) behavior of aggregates and their momentum transfer behavior. Indeed, a near equality between the effective scavenging radius and the mobility equivalent radius has been reported and discussed by Meakin et al. (1989), Schmidt-Ott et al. (1990), and Rogak et al. (1991) (who report agreement within ca. 15% for $Kn \leq O(1)$). This implies that our scavenging rate formalism for aggregates, at least in the high α limit, provides some insight as to the mobility and hence Brownian diffusivity, of such aggregates over a wide range of sizes and Kn_{2R_1}-values. In view of the simplicity and computational efficiency of our methods these implications certainly warrant future investigation.

Defence of Approximations, Generalizations

It would be prudent to briefly reconsider some of our fundamental approximations, indicating their expected domain of validity and suggesting possible generalizations of likely future interest.

Continuum approximation for small N and D_f

Even though the simple scaling law: $d \ln N / d \ln r = \text{const.} \equiv D_f$ has been found to apply down to remarkably small aggregate sizes (Schmidt-Ott et al., 1988, 1990; Megaridis and Dobbins, 1990) clearly, our pseudo-continuum mathematical model (in which each aggregate is treated as a quasi-spherical porous object) should not be expected to apply to aggregates containing, say, less than about 30 primary particles. While the extent to which such pseudo-continuum results match small N detailed particle-level diffusional simulations (Rosner et al., 1991; Mackowski, 1994) remains to be investigated, we should therefore not expect our present results to be quantitatively accurate for aggregate sizes much below about 10^2, especially when D_f is less than 2. [The situation here is quite similar to our earlier theoretical studies of the evaporative combustion of a "cloud" containing N dispersed fuel droplets (Labowsky and Rosner, 1978). In anticipation of relevant "small N" results we have deliberately started our graphs at $N = 10$, in order to embrace some of the expected "matching" domain.]

Tortuosity-porosity laws over the spectrum of pore Knudsen numbers

Current research (extensions of Tassopoulos and Rosner, 1992; Melkote and Jensen, 1992; Elias-Kohav et al., 1991) may reveal that our presently used tortuosity laws are not sufficiently accurate, especially in the Knudsen pore diffusion limit (where higher-order microstructural information characterizing the likely primary sphere positions may need to be added) or in the transition regime (where the pore Knudsen number dependence of the tortuosity may not quite be monotonic and, accordingly, depart too much from the behavior tentatively assumed here). Whatever the outcome of such studies, however, the present pseudo-continuum *procedures* should remain useful to (re-)compute and correlate the accessible surface area of such aggregates as a fraction of the total area of the primary spheres present. Indeed, in the near future it would be interesting to compare the present η_{int} estimates with much more computationally-intensive Brownian simulations on computer-generated fractal aggregates in 3 dimensions.

In closing this section it should be remarked that unusual Knudsen diffusion conditions would occur deep inside such an aggregate since, as one approaches the "core" one can show that the local characteristic radial length over which the porosity changes by an appreciable fractional amount, that is, $(d \ln \epsilon / dr)^{-1}$ will no longer be large on the scale of the local average pore diameter! We should also comment that the limit $\alpha \to 1$, while formally included here, should also be expected to be singular for Knudsen diffusion (when $\alpha = 1$ no reagent molecule survives *one* collision with the pore wall!). This implies that corrections to Eq. 8 should be introduced in the high reaction probability limit (Verhoff and Streider, 1971).

Nonspherical aggregate shapes

It has been reported that "small" aggregate-aggregate encounters lead to larger aggregates for which the gyration radii are not the same in all directions. Botet and Jullien (1986) and Hentschel (1984) report an asymptotic gyration radius ratio of ca. 2. Moreover, electron micrographs of soots sampled from diverse systems usually reveal a wide variety of nonspherical aggregate morphologies, often somewhat stringy in character (Ulrich, 1984; Lahaye and Prado, 1981). While there is ample precedent for treating the effectiveness of nonspherical porous catalyst pellets (with $D_f = 3$) using the notion of an *equivalent sphere* of effective radius:

$$R_{\text{eff}} = 3 \cdot (V/A)_{\text{outer envelope}} \tag{47}$$

(See Aris, 1957). If increased accuracy were needed the present model could readily be generalized to deal with, say, prolate spheroidal porous media which are fractal-like in each principal direction. Moreover, external diffusion layer transport could be dealt with using the dimensionless transfer coefficient for such spheroids (Yovanovich, 1987) but preferably based on the characteristic length $(A_{\text{ext}}/\pi)^{1/2}$. These generalizations would allow for the fact that the characteristic Brownian *rotation* time of such large aggregates, for example, $(6D_{N,\text{rot}})^{-1}$, would be much larger than the characteristic time $((A_{\text{ext}}/\pi)/Nu_m)^2/D_{A\text{-mix}}$ for reactant molecule diffusion across the external boundary layer, especially at small Knudsen numbers based on the length $(A_{\text{ext}}/\pi)^{1/2}$. Thus, the often-quoted notion that Brownian rotation would *ensure* the reasonableness of a quasi-spherical aggregate approximation even for large elongated aggregates is probably illusory. However, we leave such generalizations to the future, noting only that some of the features of porous suspended particles which are distributed with respect to both size N and *aspect ratio* $\mathcal{AR}$ are treated in Rosner and Tandon (1994).

Kinetic laws other than first-order irreversible

As mentioned earlier, the present treatment for η_{int} and η_{overall} can be generalized to apply equally well to simple *physical* phenomena such as reversible *condensation* or *evaporation* in which the interfacial rate process (sink strength) is proportional to $\alpha\,[n_A - n_{A,\text{eq}}\{T_w;\, p\}]$ where α is now the condensation or evaporation coefficient. However, in some systems the dependence of α and $n_{A,\text{eq}}\{T_w;\, p\}$ on the radius (of curvature) of the primary particles may have to be explicitly taken into account. More complex *nonlinear* kinetic laws will require separate treatment and will inevitably reveal a dependence on additional dimensionless parameters, as is already familiar in the field of heterogeneous catalysis (Aris, 1975; Satterfield, 1970; Froment and Bischoff, 1979; Engasser and Horvath, 1973).

Primary sphere surface roughness and/or internal porosity

Using X-ray scattering or adsorption techniques some aggregated soot systems have been reported to exhibit significant primary particle surface roughness and/or porosity within the primary spherules (Lahaye and Prado, 1981; Hurd et al., 1987). If necessary, such behavior could be modeled by imagining the primary particles to consist of an outer microporous layer covering an impermeable core, or containing micropores throughout. Indeed, in the spirit of self-similarity (Feder, 1988; Dimotakis, 1991), what we have called the primary particles could themselves be viewed as fractal microspheres, thereby making direct use (on a smaller scale) of the concepts described here. From this vantage point our present treatment (As-

sumption A3) is therefore seen to be equivalent to assuming that the primary spheres are themselves characterized by an effective primary sphere Thiele modulus so large that *their* internal effectiveness factors are very small, corresponding to reaction or trapping on their outer surfaces.

Nonisothermal behavior

Since most of the interfacial processes mentioned above (physical condensation/evaporation, reactive growth from the vapor phase, oxidation (gasification) by one or more reagents in the vapor phase) are not ergoneutral; in general there will be a tendency for the aggregate to overheat or undercool relative to the surrounding gas mixture. Moreover, if the effective *Biot number*, Bi_h, for radial energy transfer defined by:

$$Bi_h \equiv (k_g/k_{agg,eff}) \cdot (Nu_h/2) \tag{48}$$

(Rosner, 1986, 1990) is not sufficiently small, then temperature nonuniformities *within* the aggregate may play a role in determining both η_{int} and $\eta_{overall}$, especially when the reaction probability α is low and sharply (Arrhenius-) temperature dependent, and the mole fraction of the reagent is not very small. [In this case it might also be necessary to account for the tendency, due to radiative energy loss, for the larger aggregates to be systematically cooler than the smaller ones (Mackowski et al., 1991, 1994; Rosner et al., 1992).]

At the moment, not enough is known about the local effective radial thermal conductivity, $k_{agg,eff}$, within such aggregates, including the Rayleigh-limit *radiative* contribution, to realistically assess these nonisothermal effects. However, we remind the reader that, under thermophysical conditions such that $Bi_h \ll 1$, then our *isothermal* η_{int}-results (Figures 7 and 8) *could* be taken over to find $\eta_{overall}$ even under nonisothermal conditions, since the dominant temperature nonuniformities would then occur only in the external (thermal) gaseous boundary layer.

Conclusions

Principal conclusions for $D_f < 3$ aggregates

A simple pseudo-continuum method has been developed, described and illustrated for calculating the accessible surface area of a large open aggregate containing N primary spherical particles ($N \gg 1$) suspended in a gas at pressures such that the mean-free-path is not necessarily negligible or appreciable compared to the overall aggregate radius. For this purpose, the N-particle aggregate has been treated as a porous granular solid characterized by the scaling exponent $D_f = d\ln N/d\ln r$, and the primary sphere diameter $2R_1$. A simple yet rational correlation scheme has been developed, based on the more familiar $D_f = 3$ case and the notion of an effective (stretched) Thiele modulus Φ_{eff}, which can predict to within about 3% the numerically calculated normalized accessible surface area of such an aggregate over the entire range of parameters of physical interest, viz.: primary particle number, N; structural exponent, D_f; reaction probability, α; and Kn_{2R_1}, the ambient gas mean-free-path (measured in primary particle diameters). As a byproduct, valuable insight has been provided on recent experimental techniques for *in situ* probing of the accessible area of fractal aggregates, for example, the scavenging of radioactive lead atoms and photoelectron emission.

Application of correlations to a'''_{eff} calculations for coagulation-aged suspensions

This formulation and the above-mentioned correlation open the door to calculations of the accessible area per unit volume for coagulation-aged *populations* of aggregates, as observed in many technologies, and in natural environments. Thus, if there are a total of N_p aggregates per unit volume, with specified normalized *size distribution* $pdf\{N\}$, we can now rapidly calculate (at least for, say, $N \geq 30$) the most difficult part of the integrand appearing in:

$$a'''_{eff} = N_p \cdot \int_1^\infty a_1 N \cdot \eta_{overall}\{N;\ D_f,\ \alpha,\ Kn_{2R_1}\} \cdot pdf\{N\}\, dN \tag{49}$$

and compare the result of this integration to the total area per unit volume, a'''_{max}, associated with the sum of all primary particles present *irrespective of their state of aggregation*. Indeed, this a'''_{eff}/a'''_{max}-ratio, which can be considered an *overall effectiveness factor for the aggregate population*, will be seen to dictate aggregated particle/carrier fluid exchange processes in many applications involving flocculated suspensions (Rosner and Tandon, 1993a), including physical- and chemical-vapor deposition (Castillo and Rosner, 1988; Rosner and Liang, 1987) and "particle-modified" chemical vapor deposition (Komiyama et al., 1991).

Future work on transport to/from large aggregates

A number of the generalizations outlined in the fourth section may prove to be necessary and ultimately valuable, building on the effective porous object results and approach outlined here. Indeed, to better understand the large N-limit this approach is being extended to *all* interesting mass-, momentum-, and energy exchange properties of aggregates, including their thermophoretic "propulsion" (Rosner et al., 1991) and radiative properties (Dobbins and Megaridis, 1991; Mackowski, 1992b). It would also be interesting to investigate the vapor nucleating ability of such aggregates, including uptake rates by capillary condensation in the singular "pores" created where primary particles touch. These investigations of aggregates containing many primary spherical particles, including their rearrangement (restructuring) kinetics (Cohen and Rosner, 1994) are now underway, using some of the results of this article and analogous pseudo-continuum methods (Rosner, Cohen, and Tandon, 1993).

Acknowledgments

It is a pleasure to acknowledge the financial support of DOE-PETC (under Grant DE-FG22-90PC90099) and the US AFOSR (under Grant AFOSR 91-0170), as well as the related support of the Yale HTCRE Laboratory by our *Industrial Affiliates* (Shell, General Electric Co., and Dupont). The authors have also benefited from the perceptive comments of G. Mulholland, R. Santoro, J. Fernandez de la Mora, J. O'Brien, R. D. Cohen, and J. Rosell.

Notation

a_1 = surface area of one primary sphere (Figure 2)
a''' = surface area per unit volume
A = reactant species [OH(g), C_2H_2(g), ^{211}Pb(g)], or area
$\mathcal{AR}$ = aspect ratio (of prolate spheroid)

Bi_h = Biot number for heat-transfer (ratio of internal- to external heat-transfer resistance)
c = normalized species A local concentration variable
$\bar{c}_A$ = mean thermal speed of molecules A, $[8k_BT/(\pi m_A)]^{1/2}$
D = normalized effective diffusion coefficient; Eqs. 2-18
$D_{A,\mathrm{eff}}$ = effective diffusion coefficient for species A in local porous medium
$D_{A\text{-mix}}$ = coefficient for diffusion of species A through prevailing vapor mixture
D_f = fractal dimension, exponent $d\ln N/d\ln r$
D_K = Knudsen diffusion coefficient (single straight pore of average diameter)
f = fraction of incident molecules scattered diffusely (by surface)
k'''_{eff} = effective pseudo-homogeneous first-order rate constant $(k''a''')$
k'' = first-order heterogeneous rate constant
k_B = Boltzmann constant
Kn = Knudsen number (ratio of gas mean-free-path to characteristic dimension)
l = gas mean-free path
m_a = molecular mass of species A
n_A = local number of density of species A
N = total number of primary spheres in aggregate (see Figure 2)
Nu_m = Nusselt (Sherwood) number for mass transfer to/from sphere
r = radius (measured from aggregate center-of-mass); Figure 2
R_1 = radius of primary spheres; Figure 2
R_c = inner core radius; Eq. 3
R_{gyr} = radius of gyration; Figure 2
$R_{\max}$ = maximum (outer) radius defined by Eq. 4
T_w = absolute temperature of solid at $r=R_{\max}$
V = volume
x = argument (of the indicated function): $\eta_3\{x\}$

Greek letters

α = reaction probability, condensation coefficient, and so on $(0\le\alpha\le 1)$
β = filling factor (Eq. 2) $=\phi_{\lim}=1-\epsilon_{\lim}$
ϵ = local void fraction $(1-\phi)$
ζ = normalized radial position variable, $r/R_{\max}$
η = "effectiveness" factor: accessible area as a fraction of Na_1
$\eta_3\{x\}$ = function defined by Eq. 31
λ = radiation wavelength
τ = tortuosity of local pore structure defined by Eqs. 6 and 7
Φ = Thiele modulus (reciprocal of dimensionless reactant penetration depth)
ϕ = solid fraction $(1-\epsilon)$

Miscellaneous

BC = boundary condition
cm = center of mass; Figure 2
FAM = finite-analytic method
ODE = ordinary differential equation
$O\{\ \}$ = order of magnitude "operator"
S-O = Schmidt-Ott
$\tanh\{\ \}$ = hyperbolic tangent function
^{211}Pb = radioactive isotope of the element lead
$(\tilde{\ })$ = normalized by conditions at $r=R_{\max}$
$\langle\ \rangle_q$ = average value defined by Eq. 33
$\{\ \}$ = argument of indicated function
$fct\{\ \}$ = function of indicated argument
$pdf\{\ \}$ = probability density function of indicated random variable

Subscripts

agg = pertaining to aggregate
A = pertaining to species A
c = pertaining to core or to continuum (high-pressure limit) conditions
eff = effective
eq = pertaining to local equilibrium
exp = experimental
ext = external
f = fractal
gyr = gyration
h = pertaining to heat transfer
int = internal
K = Knudsen
lim = limiting value
m = pertaining to mass transfer
mix = pertaining to local vapor mixture
max = maximum value
pore = based on (mean) pore diameter
q = index appearing in Eq. 33; $q\ge 0$
rot = rotational
$2R_1$ = based on diameter of primary particles
1 = primary particle (spherule); Figure 2
∞ = evaluated at $r=\infty$ (far from aggregate center-of-mass)

Literature Cited

Abbasi, M. H., J. W. Evans, and I. S. Abramson, "Diffusion of Gases in Porous Solids: Monte Carlo Simulations in the Knudsen and Ordinary Diffusion Regimes," *AIChE J.*, **29**(4), 617 (1983).

Aris, R., "On Shape Factors for Irregular Particles—I. The Steady State Problem. Diffusion and Reaction," *Chem. Eng. Sci.*, **6**, 262 (1957).

Aris, R., *The Mathematical Theory of Diffusion and Reaction in Permeable Catalysts—Volume 1*, Clarendon, New York (1975).

Botet, R., "Aerodynamics of 'Filigree' Objects," in preparation (1992).

Botet, R., and R. Jullien, "Intrinsic Anisotropy of Clusters in Cluster-Cluster Aggregation," *J. Phys. A: Math. Gen.*, **19**, L907 (1986).

Burtscher, H., and A. Schmidt-Ott, "Experiments on Small Particles in Gas Suspension," *Surface Sci.*, **156**, 735 (1985).

Butt, J. B., *Reaction Kinetics and Reactor Design*, Prentice-Hall, Englewood Cliffs, NJ (1980).

Castillo, J. L., and D. E. Rosner, "Nonequilibrium Theory of Surface Deposition from Particle-Laden, Dilute Condensible Vapor-Containing Stream, Allowing for Particle Thermophoresis and Vapor Scavenging Within the Laminar Boundary Layer," *Int. J. Multiphase Flow*, **14**(1), 99 (1988).

Charalampopoulos, T. T., and H. Chang, "Agglomerate Parameters and Fractal Dimension of Soot Using Light Scattering—Effects on Surface Growth," *Combustion and Flame*, **87**, 89 (1991).

Chen, C. J., and H. C. Chen, "Finite Analytic Numerical Method for Unsteady Two-Dimensional Navier-Stokes Equations," *J. Computational Physics*, **53**, 209 (1984).

Cohen, R. D., and D. E. Rosner, "Restructuring Kinetics of Multi-Particle Aggregates," in preparation (1994).

Coniglio, A., and H. E. Stanley, "Screening of Deeply Invaginated Clusters and the Critical Behavior of the Random Superconducting Network," *Phys. Rev. Lett.*, **52**(13), 1068 (1984).

Correa, S. M., and W. Shyy, "Computational Models and Methods for Continuous Gaseous Turbulent Combustion," *Prog. in Energy and Combust Sci.*, **13**(4), 249 (1987).

Dickenson, E., "Short-Range Structure in Aggregates, Gels and Sediments," *J. Colloid Interface Sci.*, **118**(1), 286 (1987).

Dimotakis, P. E., "Fractals, Dimensional Analysis and Similarity, and Turbulence," *Nonlinear Sci. Today*, **1**(2), 1 (1991).

Dixon-Lewis, G., D. Bradley, and S. El-Din Habik, "Oxidation Rates of Carbon Particles in Methane-Air Flames," *Combustion and Flame*, **86**, 12 (1991).

Dobbins, R. A., and C. M. Megaridis, "Morphology of Flame-Generated Soot as Determined by Thermophoretic Sampling," *Langmuir*, **3**, 254 (1987).

Dobbins, R. A., and C. M. Megaridis, "Absorption and Scattering of Light by Polydisperse Aggregates," *Appl. Optics*, **30**(33), 4747 (1991).

Elias-Kohav, T., and M. Sheintuch, "Steady-State Diffusion and Reactions in Catalytic Fractal Porous Media," *Chem. Eng. Sci.*, **46**(11), 2787 (1991).
Engasser, J. M., and C. Horvath, "Effect of Internal Diffusion in Heterogeneous Enzyme Systems: Evaluation of True Kinetic Parameters and Substrate Diffusivity," *J. Theor. Biol.*, **42**, 137 (1973).
Feder, J., "The Cluster Fractal Dimension," in *Fractals*, Plenum Press, New York, pp. 31-40 (1988).
Feng, H., and D. E. Rosner, "Energy Transfer Effects of Excited Molecule Production by Surface-Catalyzed Atom Recombination," *Faraday Trans. I.—Phys. Chem.*, **70**, 884 (1974).
Formenti, M., M. Juillet, P. Meriaudeau, S. J. Teichner, and P. Vergnon, "Aerosol Route to Metal Oxide Catalysts," *J. Colloid Interface Sci.*, **39**(1), 79 (1972).
Friedlander, S. K., *Smoke, Dust and Haze—Fundamentals of Aerosol Behavior*, John Wiley, New York (1977).
Froment, G. F., and K. B. Bischoff, *Chemical Reactor Analysis and Design*, John Wiley, New York (1979).
Gomez, A., and D. E. Rosner, "Thermophoretic Effects on Particles in Counterflow Laminar Diffusion Flames," *Combust. Sci. and Tech.*, **89**, 335 (1993).
Hagenlock, R., and S. K. Friedlander, "Numerical Calculations of Collision Frequency of Molecules With DLA Clusters," *J. Colloid Interface Sci.*, **133**(1), 185 (1989).
Harris, S. J., and A. M. Weiner, "Soot Particle Growth in Premixed Toluene/Ethylene Flames," *Combust. Sci. and Tech.*, **38**, 75 (1984).
Hentschel, H. G. E., "The Structure and Fractal Dimension of Generalized Diffusion-Limited Aggregates," in *Kinetics of Aggregation and Gelation*, F. Family and D. P. Landau, eds., Elsevier, pp. 165-168 (1984).
Huizenga, D. G., and D. M. Smith, "Knudsen Diffusion in Random Assemblages of Uniform Spheres," *AIChE J.*, **32**(1), 1 (1986).
Hurd, A. J., D. W. Schaefer, and J. E. Martin, "Surface and Mass Fractals in Vapor-Phase Aggregates," *Phys. Rev.*, **A35**(5), 2361 (1987).
Israel, R., and D. E. Rosner, "Use of a Generalized Stokes Number to Determine the Aerodynamic Capture Efficiency of Non-Stokesian Particles from a Compressible Gas Flow," *Aerosol Sci. Tech.*, **2**, 45 (1983).
Julien, R., M. Kolb, and R. Botet, "Scaling Properties of Growth by Kinetic Clustering of Clusters," in *Kinetics of Aggregation and Gelation*, F. Family and D. P. Landau, eds., Elsevier, New York (1984).
Koch, W., and S. K. Friedlander, "The Effect of Particle Coalescence on the Surface Area of a Coagulating Aerosol," *J. Colloid Int. Sci.*, **140**, 419 (1990).
Komiyama, H. T., and L. S. Hong, "Chemical Vapor Deposition of CuO_x Films by CuI and O_2: Role of Cluster Formation on Film Morphology," *J. Amer. Ceram. Sci.*, **74**(7), 1597 (1991).
Labowsky, M., and D. E. Rosner, "Group Combustion of Droplets in Fuel Clouds: I. Quasi-Steady Predictions," *Evaporation—Combustion of Fuels: ACS Advances in Chem. Series*, **166**, 63 (1978).
Lahaye, J., and G. Prado, "Morphology and Internal Structure of Soot and Carbon Blacks," in *Particulate Carbon: Formation During Combustion*, D. C. Siegla and G. W. Smith, eds., Plenum Press, New York, pp. 33-55 (1981).
Mackowski, D. W., "Phoretic Behavior of Asymmetric Particles in Thermal Nonequilibrium with the Gas: Two Sphere Aggregate," *J. Colloid Int. Sci.*, **140**(1), 138 (1990).
Mackowski, D. W., M. Tassopoulos, and D. E. Rosner, "Effect of Radiative Heat Transfer on the Coagulation Rates of Combustion-Generated Particles," *Aerosol Sci. Tech.*, **20**(1), 83 (1994).
Matijevic, E., "Monodispersed Metal (Hydrous) Oxides—A Fascinating Field of Colloid Science," *Acc. Chem. Res.*, **14**, 22 (1981).
Matsoukas, T., and S. K. Friedlander, "Dynamics of Aerosol Agglomerate Formation," *J. Colloid Interface Sci.*, **146**(2), 495 (1991).
Meakin, P., and T. A. Witten, Jr., "Growing Interface in Diffusion-Limited Aggregation," *Phys. Rev.*, **A28**(5), 2985 (1983).
Meakin, P., "Particle-Cluster Aggregation With Fractal Particle Trajectories and On Fractal Substrates," in *Kinetics of Aggregation and Gelation*, F. Family and D. P. Landau, eds., Elsevier, pp. 91-99 (1984).
Meakin, P., B. Donn, and G. W., Mulholland, "Collisions Between Point Masses and Fractal Aggregates," *Langmuir*, **5**, 510 (1989).
Medalia, A. I., and F. A. Heckman, "Morphology of Aggregates—II. Size and Shape Factors of Carbon Black Aggregates from Electron Microscopy," *Carbon*, **7**, 567 (1969).
Megaridis, C. M., and R. A. Dobbins, "Morphological Description of Flame-Generated Materials," *Combust. Sci. Tech.*, **71**, 95 (1990).
Melkote, R. R., and K. F. Jensen, "Computation of Transition and Molecular Diffusivities in Fibrous Media," *AIChE J.*, **38**(1), 56 (1992).
Mohamed, R. S., P. G. Debenedetti, and R. K. Prud'homme, "Effects of Process Conditions on Crystals Obtained from Supercritical Mixtures," *AIChE J.*, **35**(2), 325 (1989).
Mountain, R. D., and G. W. Mulholland, "Stochastic Dynamics Simulation of Particle Aggregation," in *Kinetics of Aggregation and Gelation*, F. Family and D. P. Landau, eds., Elsevier, pp. 83-86 (1984).
Mountain, R. D., G. W. Mulholland, and H. R. Baum, "Simulation of Aerosol Agglomeration in the Free-Molecular and Continuum Flow Regimes," *J. Colloid Interface Sci.*, **114**(1), 67 (1986).
Mountain, R. D., and G. W. Mulholland, "Light Scattering from Simulated Smoke Agglomerates," *Langmuir*, **4**, 1321 (1988).
Mulholland, G. W., R. J. Samson, R. D. Mountain, and M. H. Ernst, "Cluster Size Distribution for Free-Molecular Agglomeration," *Energy and Fuels*, **2**, 481 (1988).
Neoh, K. G., J. B. Howard, and A. F. Sarofim, "Soot Oxidation in Flames," in *Particulate Carbon: Formation During Combustion*, D. C. Siegla and G. W. Smith, eds., Plenum Press, New York, pp. 261-282 (1981).
Olague, N. E., D. M. Smith, and M. Ciftcioglu, "Knudsen Diffusion in Ordered Sphere Packings," *AIChE J.*, **34**(11), 1907 (1988).
Puri, R., T. F. Richardson, R. J. Santoro, and R. A. Dobbins, "Aerosol Dynamic Processes of Soot Aggregates in a Laminar Ethene Diffusion Flame," *Combustion and Flame*, **92**(3), 320 (1993).
Rogak, S. N., and R. C. Flagan, "Stokes Drag on Self-Similar Clusters of Spheres," *J. Colloid Interface Sci.*, **134**(1), 206 (1990).
Rogak, S. N., U. Baltensperger, and R. C. Flagan, "Measurement of Mass Transfer to Agglomerate Aerosols," *Aerosol Sci. Tech.*, **14**, 447 (1991).
Rogak, S. N., H. V. Nguyen, and R. C. Flagan, "The Mobility and Structure of Aerosol Agglomerates," *Aerosol Sci. Tech.*, **18**, 25 (1993).
Rosner, D. E., and M. Tassopoulos, "Deposition Rates from 'Polydispersed' Populations of Arbitrary Spread," *AIChE J.*, **35**(9), 1497 (1989).
Rosner, D. E., "High Temperature Gas-Solid Reactions," *Ann. Rev. of Mat. Sci.*, **2**, 573 (1972).
Rosner, D. E., *Transport Processes in Chemically Reacting Flow Systems*, Butterworths-Heinemann, Stoneham, MA (1990).
Rosner, D. E., R. D. Cohen, and P. Tandon, "Development of Pseudo-Continuum Theories of the Restructuring Kinetics of Large Multi-Particle Aggregates in Combustion Systems," Abstract 8D4, p. 331, AAAR Annual Meeting, Oak Brook, IL (Oct. 11-15, 1993).
Rosner, D. E., and B. Liang, "Laboratory Studies of Binary Salt CVD in Combustion Gas Environments," *AIChE J.*, **33**(12), 1937 (1987).
Rosner, D. E., D. W. Mackowski, and P. Garcia-Ybarra, "Size- and Structure-Insensitivity of the Thermophoretic Transport of Aggregated 'Soot' Particles in Gases," *Combust Sci. Tech.*, **80**(1-3), 87 (1991).
Rosner, D. E., D. W. Mackowski, M. Tassopoulos, and P. Garcia-Ybarra, "Effects of Heat Transfer on the Dynamics and Transport of Small Particles in Gases," *Ind./Eng. Chem.-Research*, **31**, 760 (1992).
Rosner, D. E., R. Nagarajan, M. Kori, and S. A. Gokoglu, "Maximum Effect of Vapor Phase Chemical Reactions on CVD-Rates and Deposition Onset Conditions in the Absence of Interfacial Chemical Kinetic Barriers," *Proc. 10th Inf. Conf. on CVD*, G. W. Cullen, ed., The ElectroChem Soc., **87-8**, pp. 61-80 (1987).
Rosner, D. E., and P. Tandon, "Effective Area/Volume and Sorptive Capacity of Populations of 'Microporous' Aerosol Particles Distributed With Respect to Both Size (Volume) and Shape," *AIChE J.*, submitted (1994).
Rosell, J., "Vapor Scavenging Ability of a Fractal Aggregate," *Yale University, ChE 620a Course Report* (1990).
Roth, P., O. Brandt, and S. Von Gersum, "High Temperature Oxidation of Suspended Soot Particles Verified by CO and CO_2 Measurements," *23rd Int. Symposium on Combustion*, Orleans, France, The Combustion Institute, pp. 1485-1491 (1990).

Satterfield, C. N., *Mass Transfer in Heterogeneous Catalysis*, MIT Press, Cambridge, MA (1977).
Schaefer, D. W., E. J. Martin, P. Wiltzins, and D. S. Cannell, "Fractal Geometry of Colloidal Aggregates," *Phys. Rev. Lett.*, **52**, 2371 (1984).
Schaefer, D. W., "Fractal Models and Structure of Materials," *MRS Bulletin*, **8**(2), 22 (1988).
Schaefer, D. W., A. J. Hurd, D. K. Christen, S. Spooner, and J. S. Lin, "Growth and Structure of Pyrogenic Silica," *Mat. Res. Sci. Symp. Proc.*, **121**, 305 (1988).
Schmidt-Ott, A., "*In Situ* Measurement of the Fractal Dimensionality of Ultrafine Aerosol Particles," *Appl. Phys. Lett.*, **52**(12), 954 (1988).
Schmidt-Ott, A., "New Approaches to *In Situ* Characterization of Ultrafine Agglomerates," *J. Aerosol Sci.*, **19**(5), 553 (1988).
Schmidt-Ott, A., U. Baltensperger, H. W. Gaggeler, and D. T. Jost, "Scaling Behaviour of Physical Parameters Describing Agglomerates," *J. Aerosol Sci.*, **21**(6), 711 (1990).
Sheintuch, M., and S. Brandon, "Deterministic Approaches to Problems of Diffusion, Reaction and Adsorption in a Fractal Porous Catalyst," *Chem. Eng. Sci.*, **44**(1), 69 (1989).
Siegla, D. C., and G. W. Smith, eds., *Particulate Carbon: Formation During Combustion*, Plenum Press, New York (1981).
Smith, D. M., "Knudsen Diffusion in Constricted Pores: Monte-Carlo Simulations," *AIChE J.*, **32**(2), 329 (1986).
Tassopoulos, M., and D. E. Rosner, "Simulation of Vapor Diffusion in Anisotropic Particulate Deposits," *Chem. Eng. Sci.*, **47**(2), 421 (1991).
Torquato, S., "Thermal Conductivity of Disordered Heterogeneous Media from the Microstructure," *Rev. in Chem. Eng.*, **4**, 151 (1984).
Torquato, S., "Random Heterogeneous Media; Microstructure and Improved Bounds on Effective Properties," *Appl. Mech. Rev.*, **44**(2), 37 (1991).
Ulrich, G. D., "Flame Synthesis of Fine Particles," *Chem. Eng. News (ACS)*, 22 (1984).
Verhoff, F. H., and W. Streider, "Numerical Studies of Knudsen Diffusion and Chemical Reaction in Capillaries of Finite Length," *Chem. Eng. Sci.*, **26**, 245 (1971).
Wu, M. K., and S. K. Friedlander, "Enhanced Power-Law Agglomerate Growth in the Free-Molecule Regime," *J. Aerosol Sci.*, **24**(3), 273 (1993).
Yovanovich, M. M., "New Nusselt and Sherwood Numbers for Arbitrary Isopotential Bodies at Near Zero Peclet and Rayleigh Numbers," Paper No. AIAA-87-1643, *AIAA 22nd Thermophysics Conf.*, Honolulu (June, 1987).
Zukoski, C. F., M. K. Chow, G. H. Bogush, and J. L. Look, "Precipitation of Uniform Particles—The Role of Aggregation," *Mat. Res. Soc. Symp. Proc.*, **180**, 131 (1990).

Manuscript received Oct. 14, 1992, and revision received Oct. 4, 1993.